

# Multiband theory of quantum-dot quantum wells: Dark excitons, bright excitons, and charge separation in heteronanostructures

W. Jaskólski\* and Garnett W. Bryant

*National Institute of Standards and Technology, Gaithersburg, MD 20899, USA*

*e-mail: garnett.bryant@nist.gov*

(Current version dated October 4, 2018)

## Abstract

Electron, hole, and exciton states of multishell CdS/HgS/CdS quantum-dot quantum well nanocrystals are determined by use of a multiband theory that includes valence-band mixing, modeled with a 6-band Luttinger-Kohn Hamiltonian, and nonparabolicity of the conduction band. The multiband theory correctly describes the recently observed dark-exciton ground state and the lowest, optically active, bright-exciton states. Charge separation in pair states is identified. Previous single-band theories could not describe these states or account for charge separation.

PACS numbers: 71.35.-y, 73.23.-b, 73.61.-r, 78.20.-e

Quantum-dot quantum well (QDQW) nanocrystals are composed of an internal semiconductor core which is coated with several shells of different semiconductors [1,2]. These structures have been synthesized by wet chemistry and can have spherical [3] or tetrahedral [1] shape. The method of covering CdS or HgS nanocrystals by HgS or CdS shells has been established for several years [4]. Recently, QDQWs containing three layers, each with a thickness controlled to a single monolayer [3,5], have been fabricated. Transition energies and optical dynamics in these structures can be precisely designed by changing the internal core diameter and thickness of each shell. With the possibility of achieving very uniform size distributions of dots in a sample and the ability of forming 2D and 3D arrays of chemically synthesized nanocrystals [6], QDQWs become intriguing candidates as building blocks in QD arrays for novel electronic and optical applications.

Recently Mews *et al.* [1] have fabricated and studied QDQW nanocrystals formed with 4-5 nm diameter CdS cores, 1 ML HgS shells, and  $\sim 2$  nm wide CdS outer cladding layers. Since CdS has a wide band gap and HgS has a narrow band gap, the radial profiles for conduction band (CB) and valence band (VB) edges of a CdS/HgS/CdS QDQW each form an internal quantum well in the HgS layer. The electron-hole excitations in these structures are determined by competition between global confinement in the entire nanocrystal, local confinement in the internal quantum well, and electron-hole pair interaction.

The low energy optical excitations in these QDQWs have been measured by absorption, luminescence, fluorescence line narrowing (FLN), and hole burning (HB) [1]. The lowest optically active electron-hole pair state is separated from the next optically active pair state by about 60 meV. A large, 19 meV Stokes energy shift is observed between the lowest optically active pair state, that is used as the excitation level in the fluorescence measurements, and the main emission peak, indicating that the ground state is a *dark* exciton.

Electron, hole, and exciton states of QDQWs have been investigated so far only with the one-band effective mass approximation, treating a light hole with a mass similar to the CB mass [2,3,7]. The energy of the main absorption peak can be predicted reasonably well by these calculations. However, in these calculations, the main absorption peak arises from

transitions to the lowest pair state, there is no dark-exciton ground state. Also, the next optically active pair state is predicted to be 200 meV above the lowest optically active state. Since the electron and hole have similar masses in these models, little separation of the electron and hole into different layers is predicted.

The presence of multiple, closely spaced excitations with very different oscillator strengths suggests that a more detailed description of the band states, including both heavy and light holes, is needed for these QDQWs. It has been proved for other semiconductor quantum dots [8–11] that valence-band mixing must be included to correctly describe hole levels, transition energies, and excitation spectra. For structures containing layers of narrow-gap semiconductors, such as HgS, CB nonparabolicity should also be included. To explain the recently observed spectra of CdS/HgS/CdS quantum dots [1], to determine when charge separation occurs, and to study how energy levels and excitation spectra depend on CdS and HgS shell thicknesses, we have performed multiband calculations for spherical QDQWs based on the  $\mathbf{k} \cdot \mathbf{p}$  method and the envelope function approximation (EFA).

We use the 6-band Luttinger-Kohn Hamiltonian in the spherical approximation [8] to describe hole states. Only the angular momentum operator  $F = J + L$ , where  $J$  is the Bloch band-edge angular momentum (3/2 for heavy and light holes and 1/2 for the split-off band) and  $L$  is the envelope angular momentum in a spherical dot, commutes with the hole Hamiltonian. The hole states are eigenfunctions of  $F$  and  $F_z$

$$|FF_z; nL^h\rangle = \sum_{J,L \geq L^h} \sum_{J_z, L_z} \langle JJ_z LL_z; FF_z | JJ_z \rangle |nLL_z\rangle \quad (1)$$

where the  $|JJ_z\rangle$  are the appropriate Bloch band-edge states,  $\langle \mathbf{r} | nLL_z \rangle = f_{nL}(r) Y_{LL_z}(\hat{\mathbf{r}})$ , the  $f_{nL}(r)$  are radial envelope functions and the  $Y_{LL_z}(\hat{\mathbf{r}})$  are spherical harmonics. Following Ref. [9,11] the hole states are described by three quantum numbers:  $nL_F^h$ , where  $n$  is the main quantum number, and  $L^h$  is the lowest  $L$  that appears in Eq.(1) for a given  $F$ . The three different radial components  $f_{nL}(r)$  that appear for a given  $F$  are solutions of a set of second-order coupled differential equations for the radial part of the 6-band Luttinger-Kohn Hamiltonian. For each semiconductor shell this Hamiltonian depends on 3 empirical

parameters: two Luttinger parameters  $\gamma$  and  $\gamma_1$  and the split-off gap  $\Delta$ .

The electron states are products of the Bloch CB-edge state  $|S\sigma\rangle$  for an  $S$  atomic state with spin  $\sigma$  and the envelope functions  $|nL^e L_z^e\rangle$ . The one-band effective-mass radial equation is solved to determine  $f_{nL^e}(r)$ . CB nonparabolicity is included perturbatively by use of an energy-dependent mass correction defined by two empirical parameters: the energy gap  $E_g$  and  $E_p = 2V^2$ , where  $V = \langle S|p_z|Z\rangle$  is the Kane matrix element [9]. The electron and hole equations are solved numerically.

We use the following material parameters: CdS  $E_g = 2.5$  eV,  $\gamma_1 = 0.814$ ,  $\gamma = 0.307$ ,  $\Delta = 0.08$  eV,  $E_p = 19.6$  eV; HgS  $E_g = 0.2$  eV,  $\gamma_1 = 12.2$ ,  $\gamma = 4.5$ ,  $\Delta = 0.08$  eV,  $E_p = 21.0$  eV. The heavy and light hole masses resulting from the  $\gamma$ ,  $\gamma_1$  are: CdS  $m_{hh} = 5.0$ ,  $m_{lh} = 0.7$ ; HgS  $m_{hh} = 0.31$ ,  $m_{lh} = 0.047$ . These parameters are the same as or close to the corresponding values found in the literature [12–16]. The HgS band gap is taken to be positive. This is consistent with recent measurements of the HgSe band gap [17]. Based on the photoelectric thresholds for CdS and HgS [18], the CB and VB offsets are taken to be 1.45 eV and 0.85 eV, respectively, which are close to the values used in previous calculations [2,3,7]. The barriers for tunneling into water, which is the medium surrounding the QDQW, are 4 eV for both electrons and holes (photoelectric threshold in H<sub>2</sub>O is  $\approx 8$  eV) when measured from the middle of the HgS gap. The H<sub>2</sub>O masses are  $m_{hh} = m_{lh} = m_e = 1.0$  ( $\gamma_1 = 1.0$  and  $\gamma = 0.0$ ) [7]. The choice of H<sub>2</sub>O masses is not critical since the high H<sub>2</sub>O barriers prevent any significant leakage out of the QDQW. Contribution from higher electronic bands is taken into account by use of the parameter  $f = -1.0$  in the electron effective mass equation [9]. As a result the electron mass is 0.15 near the CB-edge in CdS and 0.04 for the energy range of interest in HgS, close to values found in the literature [7,13,14].

To test that the EFA can be applied to QDQW structures containing layers as thin as 1 ML, we perform first a series of calculations for wide-layer structures, for which the EFA works [9–11], and then we vary shell widths to reach the limit of thin layers. The sequence is shown in Fig. 1. We start with a CdS quantum dot with a 2 nm radius, *i. e.* a 1 nm core and a 1 nm clad (structure *a* in Fig. 1). Next, we add a HgS shell between the CdS core

and clad, starting with a 0.3 nm ( $\sim 1$  ML) shell and extending to a 2 nm shell (structure *b* in Fig. 1). Next the CdS core is reduced until the limit of a HgS/CdS quantum dot with no CdS core (structure *c*) is reached. Finally, the 1 nm wide CdS clad is eliminated to end with a 4 nm diameter HgS QD (structure *d*).

Electron and hole energies are shown in Fig. 2 for this sequence of structures. Transition energies are calculated by taking the electron-hole pair energy differences and subtracting the pair binding energy, which is determined perturbatively [19] with an average effective dielectric constant. The transition energies are presented in Fig. 3a. Oscillator strengths of the lowest transitions are shown in Fig. 3b. The oscillator strengths are calculated by averaging over all linear polarizations (*i*) of the dipole transition operator

$$\sum_{L_z^e \sigma} \sum_i \left| \sum_{F_z J_z} \langle J J_z L L_z; F F_z \rangle \langle n^e L^e L_z^e | n^h L L_z \rangle \langle S \sigma | \hat{p}_i | J J_z \rangle \right|^2 \quad (2)$$

where  $\sum_{L_z^e}$  averages over final electron states and  $\hat{p}$  is the momentum operator. Most importantly, electron and hole levels evolve smoothly as layer thicknesses are varied. Thus the EFA should be quantitatively accurate for structures with wide layers and should be qualitatively accurate and quantitatively reasonable for structures with thin layers.

As the HgS shell width increases, successive electron states become trapped in the HgS shell when their energies fall below the CdS CB-edge and their charge densities become localized in the HgS shell. Due to global confinement, electron energies increase as the CdS core or clad decreases.

In the one band approximation [2,3,7], hole and electron states behave the same way when the HgS thickness is varied, with the corresponding hole and electron states trapping in the HgS for nearly the same thickness. In the multiband approximation, hole states behave differently from electron states. A group of hole levels ( $1P_{3/2}$ ,  $1P_{1/2}$ ,  $1S_{3/2}$ ) *easily* fall below the CdS VB-edge, even for a HgS shell as thin as 1 ML ( $\sim 0.3$  nm). The corresponding charge densities are strongly localized inside the HgS (see Fig. 4). These hole states are more easily trapped than the corresponding electron states. The  $n = 2$  hole states of these symmetries trap in the HgS layer at larger widths ( $\sim 0.4 - 0.5$  nm). There is also a group of

states ( $nS_{1/2}$ ) with energies above the CdS VB-edge even for a 2 nm wide HgS shell. Their charge density maxima are located in the CdS cladding layer (see Fig. 4).

The  $1S_{1/2}$  hole state does not trap in the HgS layer because the CdS and HgS hole effective masses are so different. The  $1S_{1/2}$  state is made from light hole and split-off bands only. The HgS light hole and split-off band masses are about 15 times lighter than the corresponding CdS masses. The HgS shell acts as a barrier for the  $S_{1/2}$  state, rather than a potential well, because the hole has such a light mass and high kinetic energy in that shell. Moreover, the dominant contribution from the  $J = 3/2$  band to the lowest  $S_{1/2}$  state is made by the  $L = 2$  component [8,10]. Thus the  $S_{1/2}$  charge density maximum is in the CdS clad. In contrast,  $S_{3/2}$ ,  $P_{3/2}$  and  $P_{1/2}$  states are a mixture of heavy hole, light hole and split-off bands. The HgS heavy hole mass and the CdS light hole mass are similar, so these states can localize in the HgS well.

Localization of the hole  $1S_{1/2}$  state in the CdS clad and electron  $1S$  state in the HgS shell (see Fig. 4) explains why the oscillator strength (Fig. 3b) of the  $1S_{1/2} - 1S$  transition is about two orders of magnitude smaller than of  $1P_{3/2} - 1P$  or  $1P_{1/2} - 1P$  transitions. Including the effects of pair interaction beyond the perturbation energy shift included in our calculations would not dramatically reduce this charge separation because quantum confinement effects dominate pair binding in these small structures [7]. The binding energy of an exciton in this pair state should be smaller than in other pair states, since the electron and hole are strongly localized in different layers. The oscillator strength of the  $1S_{3/2} - 1S$  transition is even smaller than for the  $1S_{1/2} - 1S$  transition. Only the  $L = 0$  component of  $1S_{3/2}$  state yields to a non-vanishing transition dipole. In these QDQW structures this component of the hole state is negligible compared to the two  $L = 2$  components. As a consequence, the  $1S_{3/2} - 1S$  transition is optically inactive.

Finally, we perform specific calculations for the QDQW nanocrystals investigated recently by Mews *et al.* [1]. We consider a structure with a CdS core of radius 2.2 nm, 1 ML (0.35 nm) HgS shell and 2 nm wide CdS clad. The calculated energies of the first two optically allowed transitions,  $1P_{3/2} - 1P$  and  $1P_{1/2} - 1P$ , are 1.890 eV and 1.929 eV, re-

spectively. In the hole burning experiment by Mews *et al.* [1,20] the first excitation energy peak appears at 1.878 eV, only 12 meV different from the calculated energy of the lowest  $1P_{3/2} - 1P$  electron-hole pair state. The next experimentally observed excitation is  $\sim 60$  meV higher (Fig. 2 of Ref. [1]) and differs from the predicted position of  $1P_{1/2} - 1P$  state by only 10 meV. Experimentally, both transitions should be of comparable strength [20]. Our calculated oscillator strengths are almost the same for these transitions (see Fig. 3b). The calculated energy of the optically inactive  $1S_{3/2} - 1S$  transition is red-shifted from the ground  $1P_{3/2} - 1P$  transition by 18 meV in almost perfect agreement with the 19 meV difference observed between absorption and emission peaks in FLN (Fig. 2 of Ref. [1]). Thus the  $1S_{3/2} - 1S$  pair state is the *dark exciton* in this structure. The energy shift  $\Delta_{HB-FLN}$  between *excitation* peaks of HB and FLN spectra shown in Fig.2 of Ref. [1] most likely occurs because the samples contain a distribution of QDQWs. The lowest calculated transition redshifts approximately by  $\Delta_{HB-FLN}$  when the CdS core radius increases to 2.8 nm.

In conclusion, a multiband theory of electron, hole, and exciton states in QDQWs has been developed. Multiband calculations show that for some pair states, the electron and hole can be trapped in different shells, yielding weak oscillator strengths for these transitions. Other transitions can be weak even if both electron and hole are localized in the same layer. The observed energy difference between the lowest optically active transitions in CdS/HgS/CdS nanocrystals, as well as the appearance of *dark exciton* can be explained by the multiband theory. This could not be done in the one-band approximation. These results show that the EFA can be applied to interpret optical spectra of nanostructures containing layers as thin as 1 ML. For even more accurate description, corrections due to any nonspherical shape of the dots, pair exchange and correlation should be included as well.

## Acknowledgments

Support from The Fulbright Foundation and KBN project No. 2 PO3B 156 10 is gratefully acknowledged.

## REFERENCES

- [1] A. Mews, A. V. Kadavanich, U. Banin, and A. P. Alivisatos, *Phys. Rev. B* **53**, R13242 (1996).
- [2] D. Schooss, A. Mews, A. Eychmüller, and H. Weller, *Phys. Rev. B* **49**, 17072 (1994).
- [3] A. Mews, A. Eychmüller, M. Giersig, D. Schooss, and H. Weller, *J. Phys. Chem.* **98**, 934 (1994).
- [4] A. Eychmüller, A. Hässelbarth, and H. Weller, *J. Lumin.* **53**, 113 (1992).
- [5] A. Hässelbarth, A. Eychmüller, R. Eichberger, M. Giersg, A. Mews, and H. Weller, *J. Phys. Chem.* **97**, 5333 (1993).
- [6] C. R. Kagan, C. B. Murray, M. Nirmal, and M. G. Bawendi, *Phys. Rev. Lett.* **76**, 1517 (1996).
- [7] G. W. Bryant, *Phys. Rev. B* **52**, R16997 (1995).
- [8] G. B. Grigoryan, E. M. Kazaryan, Al. L. Efros, and T. V. Yazeva, *Sov. Phys. Solid State* **32**, 1031 (1990).
- [9] A. I. Ekimov, *et al.*, *J. Opt. Soc. Am. B* **10**, 100 (1993).
- [10] D. J. Norris and M. G. Bawendi, *Phys. Rev. B* **53**, 16338 (1996).
- [11] W. Jaskólski and G. W. Bryant, preprint.
- [12] C. Herman and C. Weisbuch, in *Optical Orientation*, edited by F. Meyer and B. P. Zakharchenya, (Elsevier, Amsterdam, 1984).
- [13] B. F. Bielin'kii, R. V. Garasimchuk, M. V. Kurik, and M. V. Pashovskii, *Sov. Phys. J.* **12**, 973 (1969).
- [14] Landolt-Börnstein, *Numerical Data and Functional Relationships in Science and Technology*, edited by O. Madelung, (Springer-Verlag, Berlin, 1982).



- [15] G. L. Bir and G. E. Pikus, *Symmetry and Strain-Induced Effects in Semiconductors*, Israel Program for Scientific Translations, Jerusalem, (Wiley, New York, 1975).
- [16] Not all of these parameters are well known, particularly for HgS. Our choices are best estimates from the available values.
- [17] K.-U. Gawlik, *et al.*, Phys. Rev. Lett. **78**, 3165 (1997).
- [18] A. H. Nethercot, Phys. Rev. Lett. **33**, 1088 (1974).
- [19] L. E. Brus, J. Chem. Phys. **80**, 4403 (1984).
- [20] U. Banin and A. Mews, *private communication*.

\* Permanent address: Instytut Fizyki UMK, Toruń, Poland

## FIGURES

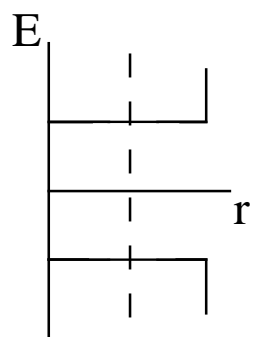
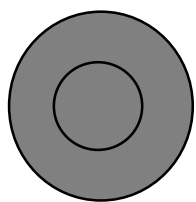
FIG. 1. The sequence of CdS/HgS/CdS quantum-dot quantum wells investigated and the corresponding schematic layout of CB and VB edges.

FIG. 2. The lowest electron (a) and hole (b) energy levels for the sequence of structures shown in Fig. 1. Left part: HgS shell increases from 0 nm to 2 nm (from left to right); middle: CdS core decreases from 1 nm to 0 nm; right: CdS clad decreases from 1 nm to 0 nm.

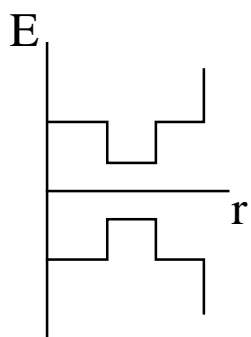
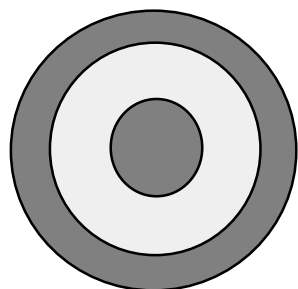
FIG. 3. Transition energies (a) and oscillator strengths (b) for the QDQW sequence in Fig. 1.

FIG. 4. Charge densities of several electron and hole states for a CdS/HgS/CdS QDQW with CdS core, radius 2.2 nm, 0.35 nm HgS shell and 2 nm CdS clad. Vertical bars mark the HgS shell.

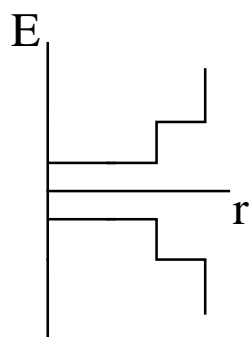
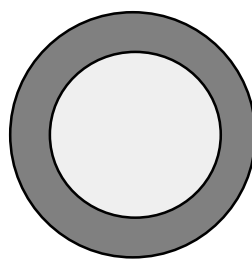
CdS



a

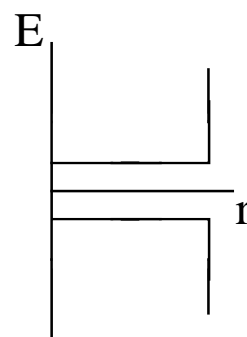
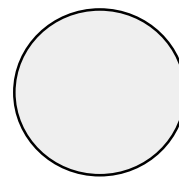


b



c

HgS



d

